Transactions of the **14th International Conference on Structural Mechanics in Reactor Technology** (SMiRT 14), Lyon, France, August 17-22, 1997

Fracture properties of carbon steel material for main primary heat transport system piping

Singh P.K., Chattopadhyay J., Kushwaha H.S.
Bhabha Atomic Research Centre, India

Abstract

The fracture mechanics calculations of Leak-Before-Break analysis of nuclear piping system require material tensile and fracture properties data. The large variation in available data may be due to variation in chemical composition and microstructure, a comprehensive program has been planned to generate material data base for primary heat transport system piping of PHWRs made of carbon steel material SA333 Gr.6. In the present paper, the tensile and fracture properties of SA333 Gr.6 material (LC orientation) evaluated at elevated temperature are described.

1. Introduction

The concept of leak before break (LBB) is used now a days to design the PHT system piping of future generation 500 MWe Indian PHWRs. *The LBB approach means the application of fracture mechanics principles to demonstrate that the pipes are highly unlikely to experience sudden catastrophic rupture without prior indication of detectable leakage.* Fracture mechanics analysis requires two basic material properties, viz. stress-strain curve and material fracture resistance curve in the form of J-R curve. Due to variation in chemical composition and heat treatment from one heat of material to another, there may be some scatter in material properties. Consequently, the United States Nuclear Regulatory Commission (USNRC) recommends to generate material properties of both base and weld metal from actual PHT system pipes at service conditions. Hence material data base generation program has been taken up. As a part of this program extensive study has been performed on tensile properties and fracture resistance properties at room temperature as well as at high temperature for SA333 Gr.6 carbon steel material.

2. Experimental details

2.1 Test Material and specimens

The carbon steel SA333 Gr.6 used in the primary heat transport system piping of 220 MWe Kaiga PHWR has been taken for preparing test specimens. The chemical composition of SA333 Gr.6 carbon steel is shown in Table 1. The round tensile specimens (fig.1) having a diameter of 3.2 mm and other dimensions conforming to ASTM standard E8M-91[2] have been used for determining tensile properties. The axis of the tensile specimen is in longitudinal direction. The compact tension specimens (fig.1) of thickness 25 mm and other dimensions conforming to ASTM standard E813-89[3] has been used for determining fracture toughness. The compact tension specimens have been cut in L-C orientation, i.e. loading is in longitudinal direction and notch is in circumferential direction of the pipe.

2.2 Tensile test method

ASTM standard E8M has been adopted for carrying out the test. The digitally controlled INSTRON 8562 servo hydraulic testing machine equipped with furnace and high temperature accessories for elevated temperature testing has been used for above study. A displacement rate of 0.003 mm/s has been used to load the specimens, under actuator control, upto fracture. Tests have been conducted at 28°C, 200°C, 250°C,and 300°C.. A computer interfaced to the testing machine was employed for the test control and the data acquisition[1].

2.3 J-integral test method

The compact tension specimen of 25 mm thickness and other dimension conforming to the ASTM standard E813 has been used for J-integral testing. Fracture toughness tests have been carried out at 28°C, 200°C, 250°C and 300°C in accordance with ASTM E813. The specimen has been pre-cracked upto a crack length to width ratio (a/w) of ~0.5 on an INSTRON 8501 servo hydraulic testing machine using a software controlled ΔK decreasing test procedure. The ΔK at the end of pre cracking was about 12 to 15 $MPa\sqrt{m}$, and the number of cycle at this stage was about 4,00,000 . The pre-cracked specimens were loaded, in the same testing machine as for tensile test. Two sets of specimens have been tested, one set without any side groove and another set with 20% side groove. A displacement rate of $3X10^{-3}$ mm/s has been employed. All specimens were fractured under fatigue loading for carrying out the post test measurements . The data has been collected at a speed of 0.5 Hz so as to have at least 30 points for calculating the crack length from loading part of the load-deflection plot using compliance crack length relations[1].

2.4 Metallography procedure

Two number of specimens of size approx. (32×28×32) mm were taken from the pipe section for study of inclusion-rating as per ASTM standard E45, grain- size measurement as per ASTM standard E112, and also to study the microstructure. The transverse and longitudinal sections of the samples were metallographically prepared and observed under microscope for inclusions. Samples were then etched with picral and then observed under microscope for grain size and microstructure.

3. Results and Discussion

3.1 Tensile Properties

The engineering stress-engineering strain plot for a typical test temperature shows that the material has prominent yield point with some amount of yield point elongation. The effect of temperature on tensile properties (Table 2) show that the ultimate tensile strength (σ_u) exhibits minimum value at 200°C and regains value better than at room temperature beyond 200°C, where as yield strength (σ_y) decrease continuously with increase in test temperature upto 300°C. The percentage elongation and percentage reduction in area has minimum value at 250°C and there after shows increasing trend. This kind of variation in tensile properties is the manifestation of embrittlement. The material does exhibit tendency towards embrittlement but loss in ductility is not substantial (5% max.) in the temperatures under consideration.

Evaluation of Ramberg-Osgood parameters

The uniaxial stress strain curve can be modeled by Ramberg-Osgood relation [7]

$\varepsilon/\varepsilon_o = \sigma/\sigma_o + \alpha(\sigma/\sigma_o)^n$; $\sigma_o = (\sigma_u+\sigma_y) / 2$; $\varepsilon_o = \sigma_o / E$

where σ_o, is reference stress (here taken as flow stress); ε_o, reference strain (σ_o/E) ; E, modulus of elasticity. The value of E has been taken as 179 GPa for higher temperatures; σ is true stress; ε is true strain; n strain hardening coefficient and α is dimensionless material constant. Since the Ramberg-Osgood coefficients α and n are sensitive to the range of true stress-true strain data the range was approximated by plotting $\log(\varepsilon_{pl})$ verses $\log(\sigma)$. The linear portion of the curve gives the range of data to be used for obtaining α and n by curve fitting. The engineering stress-engineering strain, true stress-true strain and Ramberg-Osgood curve is shown in figs.2 to 5. The values of α and n, evaluated for various test temperatures have been given in Table 2. The value of α and n obtained indicates that with increase in temperature α increases and n decreases.

3.2 Fracture toughness

For fracture toughness tests, J-R curves have been established from load-load line displacements curves and material constants C_1 and C_2 are obtained by fitting a curve using power law equation of the form,

$$J = C_1(\Delta a)^{C2}$$

where, Δa is the amount of crack extension in mm and J in KJ/m^2. The figs. 6 to 9 show test data points and fitted curve. The values of C_1 and C_2 has been shown in Table 3. The specimen thickness and J_{max} criteria given by ASTM E813 for valid J_{IC} could not be satisfied. But if component thickness is comparable to the standard specimen used in testing, the J-R curve obtained from standard specimen can be used judiciously.

Evaluation of initiation fracture toughness

The blunting line equation based on tensile properties has been evaluated according to EGG recommendation[5]. The stress-strain data obtained at same temperature as fracture toughness test has been used for evaluating blunting line. The various parameters required for evaluation of blunting line are:

(1) the ratio of yield stress and ultimate stress (σ_y/σ_μ) , (2) $\varepsilon_y = \sigma_y/E + 0.002$

(3) $\sigma_0 = \sigma_y \times 10^t$; where, $t = [n\times\log(E\times\varepsilon_y/\sigma_y)]/(n-1)$

The blunting line equation is given by,

$$\Delta a = 0.4\times d_n^* \times J/E \qquad \text{or, } J = 2.5\,(E/d_n^*)\Delta a$$

Where proportionality constant d_n^* is function of n, strain hardening exponent and σ_o/E.

The blunting line equations for different temperatures have been calculated (figs.6 to 9). Initiation fracture toughness value is the intersection of the J-R curve and the offset line parallel to blunting line at 0.15 mm. This is shown in figs.6 to 9. The fracture initiation toughness, J_i for different temperatures are given in Table 3. The Ji value decreases with increase in testing temperature, but the decrease in Ji value is not substantial. Thus it can be inferred that the loss in ductility is insignificant.

Effect of side groove

The test results for side grooved as well as non-side grooved specimens are shown in figs.10&11. The figures show that J-R curve for side grooved specimens is slightly on the higher side compared to that of non side grooved specimens. This contradicts the usual observation that putting a side groove helps in enhancing the plain strain condition and hence fracture toughness should be low. The increased J-R curve for side grooved specimens may be due to the excessive blunting of side groove (notch) because of high ductility of the material, which instead of increasing the effective thickness, has decreased it and hence reduces the constraints. The side grooved specimen has straight crack front as compared to extremely elliptical profile of non side grooved specimen.

Effect of temperature

The J-R curves for the temperatures 28°C, 200°C, 250°C and 300°C have been compared in fig. 12. The figure shows that J-R curves are identical except for 250°C which is on lower side compared to the other curves. Therefore it can be inferred that there is loss in ductility at temperature 250°C but this loss is not very significant. Again at 300°C material regains its toughness.

Evaluation of modified J-integral, J_M

Modified J-integral, J_M has been evaluated as proposed by Ernst [10]. The J_M for CT specimen is :

$$J_M = J + (1+0.76b/W)J_{pl}/b \, da$$

where, b is remaining ligament (W-a) in mm, W is width of the specimen in mm , a is crack length in mm, J_{pl} is plastic J-integral. J_M-R curves evaluated are shown in figs.13 to 16. The figures show that fracture initiation toughness J_i is same as obtained from J-R curve.

3.3 Metallography study

Transverse and longitudinal section of the sample has been prepared and observed under microscope for inclusions. Inclusions rating was done according to ASTM E112 . The inclusion rating obtained are as follows:

Inclusion type	Sulphide	Alumina	Silicate	Globular oxide
Rating	1 (thin)	1 (thin & thick ~15 micron)	1 (thin & thick ~10 micron)	1.5 (thick ~15 micron)

From above observation we find that, level of non-metallic inclusion is low which is an indication of high material toughness. The same has been observed in the fracture toughness test. The grain size measurement and microstructure study for both transverse as well as longitudinal sections shows fine grains. Towards outer diameter side grains were found to be of size ASTM grain size no. 9.5 to 10 and towards internal diameter side grain size no. 8.5 to 9 in both transverse as well as longitudinal sections. Microstructure study showed prominent banding of ferrite and pearlite towards internal diameter side in both sections and found to be gradually decreasing from internal to outer diameter side. Fig.17, shows banded structure of transverse section near internal diameter side. Very fine grain size and observed microstructural features are known to cause high toughness in the material.

4. Conclusions

The tensile and fracture property studies for SA333 Gr.6 carbon steel material at different testing temperatures can be summarized as:

1. The material shows loss of ductility and tendency towards embrittlement at 250^{0}C but loss in ductility (5% max.) is not substantial.
2. The J-R curves for side-grooved specimens are slightly on the higher side compared to non-side grooved specimens because of reduced effective thickness which in turn

produces lesser triaxiality constraint due to blunting of the side groove. The side grooved specimen is advantageous from crack length measurement point of view because of almost straight crack front.

3. The J-R curve for temperatures 28°C, 200°C, 250°C and 300°C are almost identical but for 250°C is on the lower side which again indicates embrittling of material at 250°C.
4. Fracture initiation toughness, J_i decrease with increase in testing temperature.
5. The J-R tests do not satisfy some of the ASTM validity criteria. However, since specimen thickness is comparable to component thickness, the J-R curve obtained can be used judiciously for piping analysis.
6. The chemical analysis shows low residual element content in the material which is indication of high toughness of the material. The high toughness of the material is also confirmed by the low inclusion rating and fine grain size.

Acknowledgments

This study has been supported by National Metallurgical Laboratory, Jamshedpur under Component Integrity Evaluation Program (CIEP) of Department of Atomic Energy. The authors wish to thank Dr. V.Ranganath and Dr. S.Tarafder of Material Evaluation Division of NML, Jamshedpur for carrying out tensile and fracture mechanics tests at their laboratory. The authors also thank Mr.B.K Shah (Atomic Fuel Division) & Dr. Parthasarthy (Analytical Chemistry Division) of BARC for providing useful help during the study.

References

1. Investigation on elevated temperature J-R behavior of Nuclear grade carbon steel: Report no. F&F/BARC/JR/SA333, June 1996, NML, Jamshedpur.
2. E8M-91; Standard test methods for tension testing of metallic materials; Annual book of ASTM standard, vol. 03.01, ASTM, PA, 1992, pp 150-168.
3. E813-89; Standard test methods for J_{IC}, a measure of fracture toughness; Annual book of standard, vol. 03.01, ASTM, PA, 1992, pp 732-745.
4. E1152-87; Standard test methods for determination of J-R curves; Annual book of ASTM standard; vol. 03.01, ASTM, PA, 1992, pp 847-857.
5. EGG recommendation for determination of fracture resistance of ductile materials; EGG P_I-90, December 1989, pp A5.1-A5.4.
6. W.R.Andrew, G.A.Park, P.C.Paris and D.W.Schimdt; 'Single specimen test for J_{IC} determination'; Mechanics of crack growth, ASTM-STP 590, ASTM, PA, 1976, pp 27-42.
7. D.Broek; Practical Application of fracture mechanics; pp 101.
8. Chemical analysis report; Report nos. 5255,5271,5287,5303,5329; Analytical chemistry Division, BARC.
9. Metallography evaluation of SA333 Gr.6 specimens; AFD/T1-34/96/2526; Atomic Fuel Division, BARC.
10. Ernst Hugo A. ; Material resistance and instability beyond J-controlled crack growth; ASTM/STP 803 vol.1, 1983, pp I-191-I-213.
11. Yoshida K.et.al.; Fracture toughness of weld metal in steel for NPP; Int.J.Pres.Ves. Piping 43(1990); pp 273-284

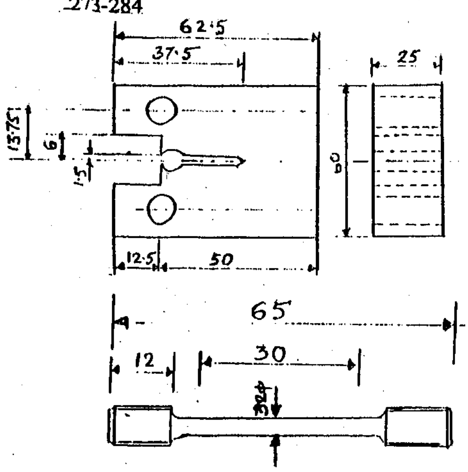

Fig-1: Sketch of compact tension specimen.
round tensile specimen.

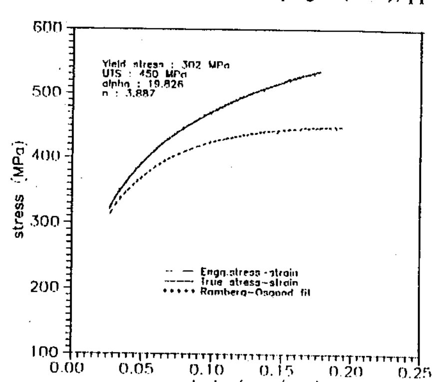

Fig-2:Stress-Strain curve for SA333 Gr.6 material at 28 deg.C

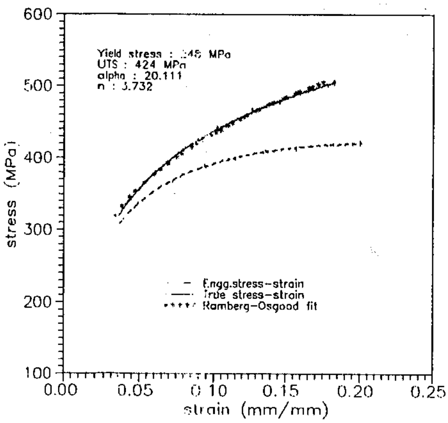

Fig-3:Stress-Strain curve for SA333 Gr.6 material at 200 deg.C

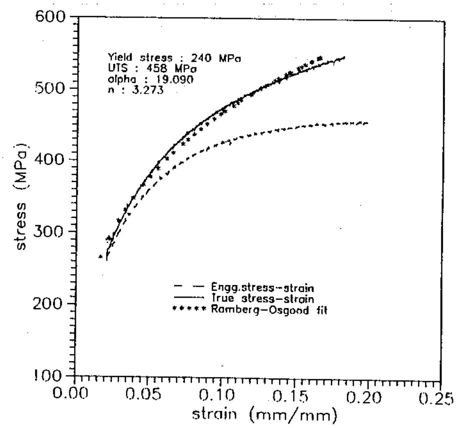

Fig-4:Stress-Strain curve for SA333 Gr.6 material at 250 deg.C

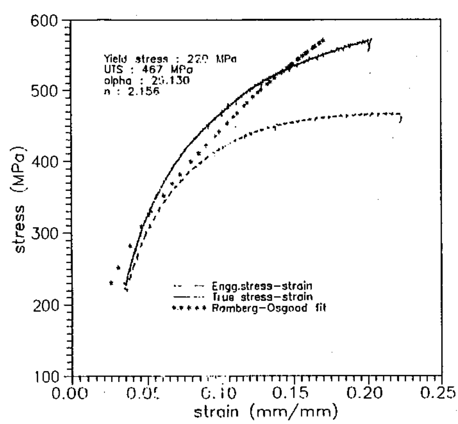

Fig-5:Stress-Strain curve for SA333 Gr.6 material at 300 deg.C

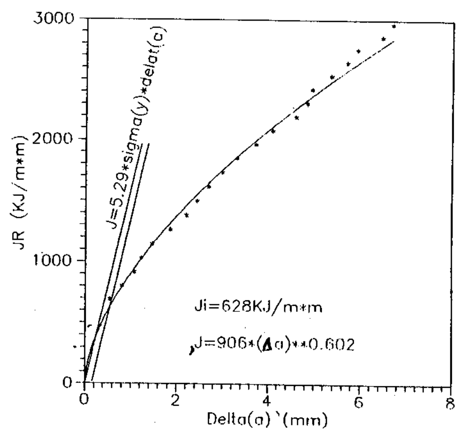

Fig-6:J-R curve of SA333 Gr6 material obtained from C-T specimens at L-C orientation at 28 deg.C

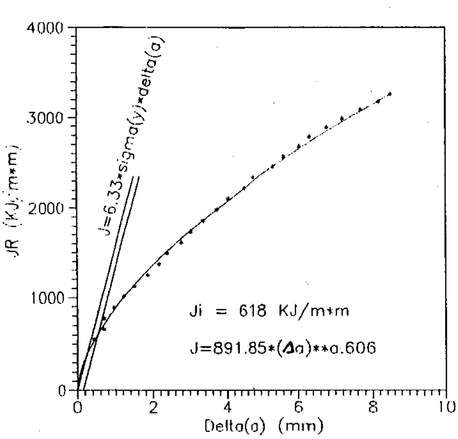

Fig-7:J-R curve of SA333 Gr6 material obtained from C-T specimens at L-C orientation at 200 deg.C

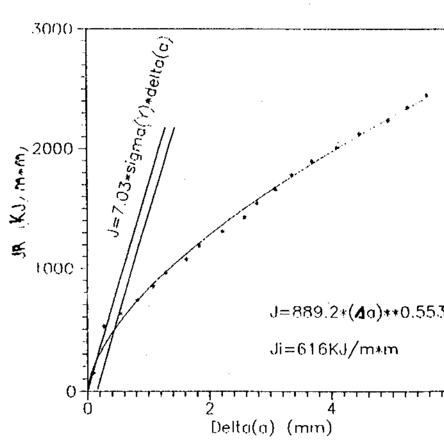

Fig-8:J-R curve for SA 333Gr.6 material obtained from C-T specimen of L-C orientation at 250 deg.C

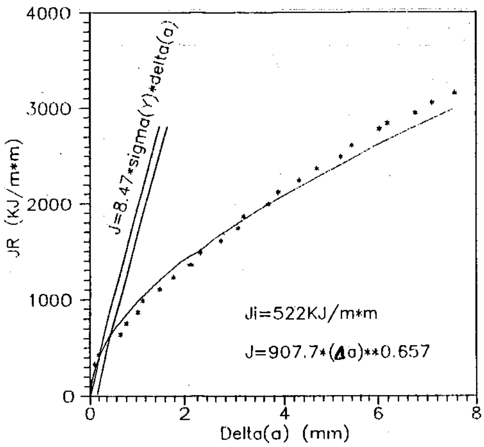

Fig-9:J-R curve for SA 333Gr.6 material obtained from C-T specimen of L-C orientation at 300 deg.C

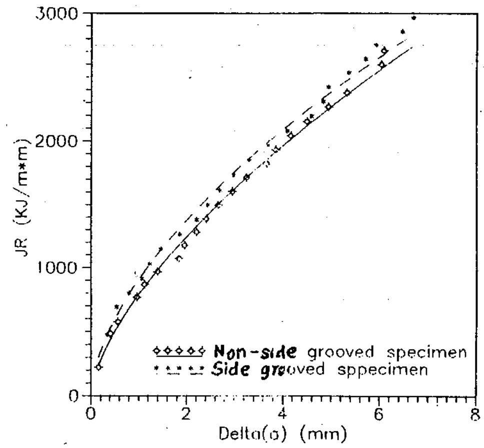

Fig-10:J-R curves for side groove and non-side grooved C-T specimens at 28 deg.C

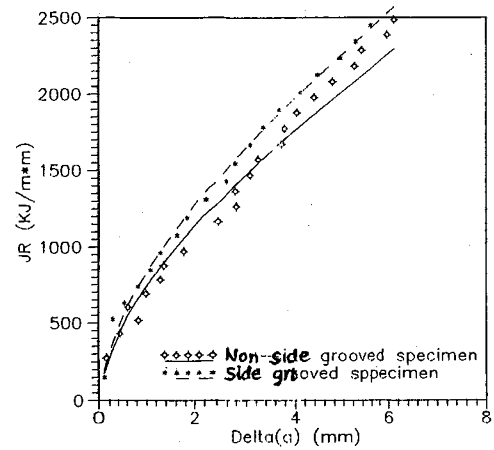

Fig-11:J-R curves for side grooved and non-side grooved C-T specimens at 250 deg.C

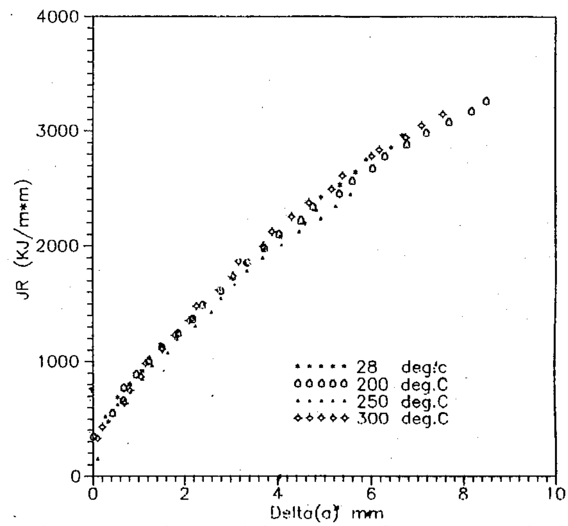

Fig-12:Comparison of J-R curve at different temperatures

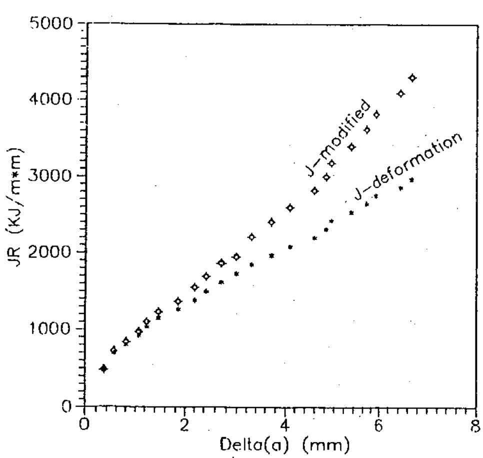

Fig-13:J-R curve of SA333 Gr6 material obtained from C-T specimens (L-C orientation) at 28 deg.C

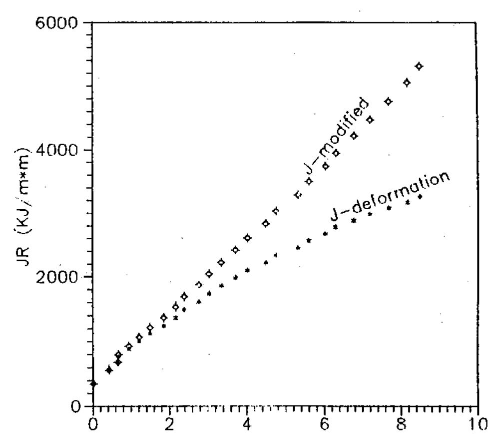

Fig-14:J-R curve of SA333 Gr6 material obtained from C-T specimens (L-C orientation) at 200 deg.C

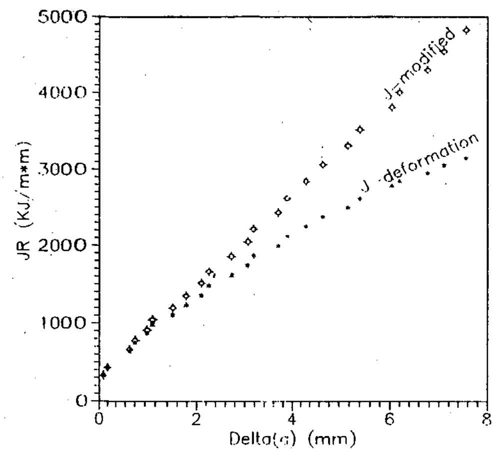

Fig-16:J-R curve of SA333 Gr6 material obtained from C-T specimens(L-C orientation) at 300 deg.C

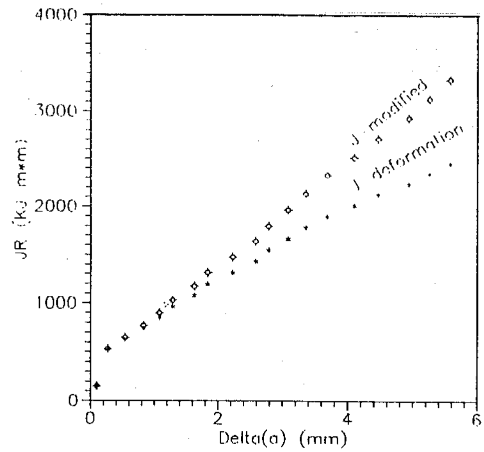

Fig-15:J-R curve of SA333 Gr6 material obtained from C-T specimens (L-C orientation) at 250 deg.C

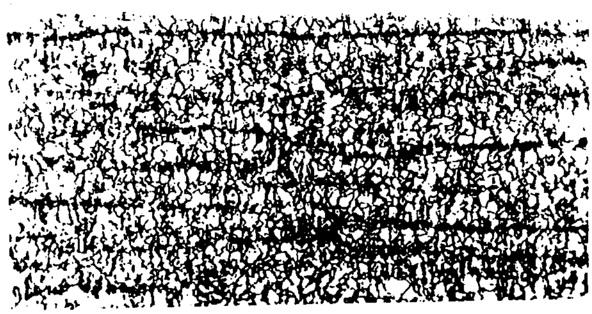

Fig-17 Photomicrograph showing fine grain (ASTM no. 9) and banded structure of ferrite and pearlite near ID side in transverse section of sample.

Table 1 : Percentage chemical composition of SA333Gr.6 carbon steel material

C	Mn	Si	P	S	Ni	Cr	N	Al	O
o.14	0.75	0.25	0.016	0.018	0.062	0.081	0.01	< 0.1	0.03

Table 2 : Tensile properties of SA 333 Gr.6 carbon steel at different temperature

Test temperature, (°C)	Yield strength, σ_y (MPa)	Ultimate strength, σ_u (MPa)	PercentageE longation	Percentage reduction in area	Ramberg - constant $\alpha^{(1)}$	Osgood $n^{(1)}$
28	302	450	36.7	72.96	19.826	3.887
200	248	424	31.4	73.23	20.111	3.732
250	240	458	29	70.57	19.090	3.273
300	220	467	34.7	72.31	29.130	2.156

(1) Ramberg-Osgood equation: $\varepsilon/\varepsilon_0 = \sigma/\sigma_0 + \alpha(\sigma/\sigma_0)^n$
where, α is dimensionless material constant ; n is strain hardening exponent ;
σ_0 is efernce stress taken as flow sterss, $(\sigma_u+\sigma_y)/2$; $\varepsilon_0 = \sigma_0/E$. E=179 GPa

Table 3 : Fracture Properties of SA333 Gr.6 carbon steel at different temperatures

Test temperature, (°C)	Power law constant, C_1	Power law constant, C_2	Initiation Fracture toughness, KJ/m^2	Constant ,m in equation of blunting line, $J=m\times\sigma_y\times\Delta a$
28	905.99	0.602	628	5.29
200	891.85	0.605	618	6.33
250	887.27	0.554	616	7.03
300	907.77	0.606	522	8.47